

# The air content of Larsen Ice Shelf

Paul R. Holland,<sup>1</sup> Hugh F. J. Corr,<sup>1</sup> Hamish D. Pritchard,<sup>1</sup> David G. Vaughan,<sup>1</sup>  
Robert J. Arthern,<sup>1</sup> Adrian Jenkins,<sup>1</sup> and Marco Tedesco<sup>2</sup>

Received 23 February 2011; revised 12 April 2011; accepted 13 April 2011; published 25 May 2011.

[1] The air content of glacial firn determines the effect and attribution of observed changes in ice surface elevation, but is currently measurable only using labor-intensive ground-based techniques. Here a novel method is presented for using radar sounding measurements to decompose the total thickness of floating ice shelves into thicknesses of solid ice and firn air (or firn water). The method is applied to a 1997/98 airborne survey of Larsen Ice Shelf, revealing large spatial gradients in air content that are consistent with existing measurements and local meteorology. The gradients appear to be governed by meltwater-induced firn densification. We find sufficient air in Larsen C Ice Shelf for increased densification to account for its previously observed surface lowering, and the rate of lowering superficially agrees with published trends in melting. This does not preclude a contribution to the lowering from oceanic basal melting, but a modern repeat of the survey could conclusively distinguish atmosphere-led from ocean-led change. The technique also holds promise for the calibration of firn-density models, derivation of ice thickness from surface elevation measurements, and calculation of the sea-level contribution of changes in grounded-ice discharge.  
**Citation:** Holland, P. R., H. F. J. Corr, H. D. Pritchard, D. G. Vaughan, R. J. Arthern, A. Jenkins, and M. Tedesco (2011), The air content of Larsen Ice Shelf, *Geophys. Res. Lett.*, 38, L10503, doi:10.1029/2011GL047245.

## 1. Introduction

[2] Satellite remote sensing provides a vital overview of ice-sheet change, but measured changes in ice surface elevation or volume discharge must be converted to mass to quantify their sea-level contributions [Zwally *et al.*, 2005; Rignot *et al.*, 2008]. This requires knowledge of the density of the ice gained or lost, for which most variation arises from firn air content. At present this can only be measured by ground-based methods, and the resulting lack of coverage means that models are commonly used [Helsen *et al.*, 2008; Shepherd *et al.*, 2010]. Here a method is presented by which depth-integrated air content may be calculated for floating ice shelves from radar sounding data, allowing the use of techniques such as airborne radio-echo sounding (RES) for which good spatial coverage is obtainable. Knowing the density at which floating ice is lost or gained also affects the attribution of the change, since surface (basal) ice is lost at the density of firn (solid ice).

[3] The method is applied to RES data from Larsen Ice Shelf (LIS). Larsen A and B (LBIS) ice shelves in the Antarctic Peninsula (AP; Figure 1a) have collapsed in recent decades in response to observed atmospheric warming [Marshall *et al.*, 2006], causing acceleration of their tributary glaciers and thus sea-level rise. The surface of Larsen C Ice Shelf (LCIS) has lowered by order 0.1 m a<sup>-1</sup> since 1992 [Shepherd *et al.*, 2003, 2010; H. D. Pritchard, manuscript in preparation, 2011, hereafter P11]. This could be caused either by a decrease in net surface accumulation or firn air content of order 0.1 m a<sup>-1</sup>, or by an increase in oceanic basal melting of order 1 m a<sup>-1</sup> (causing LCIS to sink by Archimedes' principle). The oceanography of LCIS cavity is poorly known, but basal marine ice suggests that cold waters cause relatively low melt rates [Holland *et al.*, 2009].

## 2. Method

[4] The thickness  $H$  of a hydrostatically-floating ice shelf relates to its surface elevation  $S$  above sea level by  $\rho_o(H - S) = \bar{\rho} H$ , where  $\rho_o$  and  $\bar{\rho}$  are mean densities of ocean and ice shelf. Previous studies have used thickness and elevation data to calculate  $\bar{\rho}$  and thus firn air content [e.g., Griggs and Bamber, 2009]. However, this logic is circular if the thickness is obtained by RES, because its derivation from measured radio-wave travel time requires an a-priori firn air correction. Here the problem is recast to consider the measured RES travel time and elevation, and meltwater effects are tested by considering limiting dry and saturated cases.

[5] Assuming that the total ice-shelf thickness may be decomposed into pure ice, air, and freshwater thicknesses  $I$ ,  $A$ , and  $W$ , the hydrostatic relation becomes

$$\rho_o(I + A + W - S) = \rho_i I + \rho_a A + \rho_w W, \quad (1)$$

where  $\rho_o = 1028 \text{ kg m}^{-3}$ ,  $\rho_i = 918 \text{ kg m}^{-3}$ ,  $\rho_a = 2 \text{ kg m}^{-3}$ , and  $\rho_w = 1000 \text{ kg m}^{-3}$  are densities of seawater, pure ice, and englacial air and water. This approach is pursued by applying the Complex Refractive Index Method to the RES travel time  $T$ , assuming that the dielectric permittivity is real [Arcone, 2002]:

$$T = \frac{2}{c} (In_i + An_a + Wn_w), \quad (2)$$

where  $c = 3 \times 10^8 \text{ m s}^{-1}$  is the speed of light *in vacuo* and  $n_i = 1.78$ ,  $n_a = 1.0$ ,  $n_w = 9.38$  are refractive indices of pure ice, air, and freshwater. Eliminating  $I$  from (1) and (2) gives air and water thicknesses in terms of measured and known quantities

$$\frac{cT}{2} + \frac{n_i \rho_o S}{\rho_i - \rho_o} = \left[ n_a + \frac{n_i(\rho_o - \rho_a)}{\rho_i - \rho_o} \right] A + \left[ n_w + \frac{n_i(\rho_o - \rho_w)}{\rho_i - \rho_o} \right] W. \quad (3)$$

<sup>1</sup>British Antarctic Survey, Cambridge, UK.

<sup>2</sup>Earth and Atmospheric Sciences, City College of New York, New York, New York, USA.

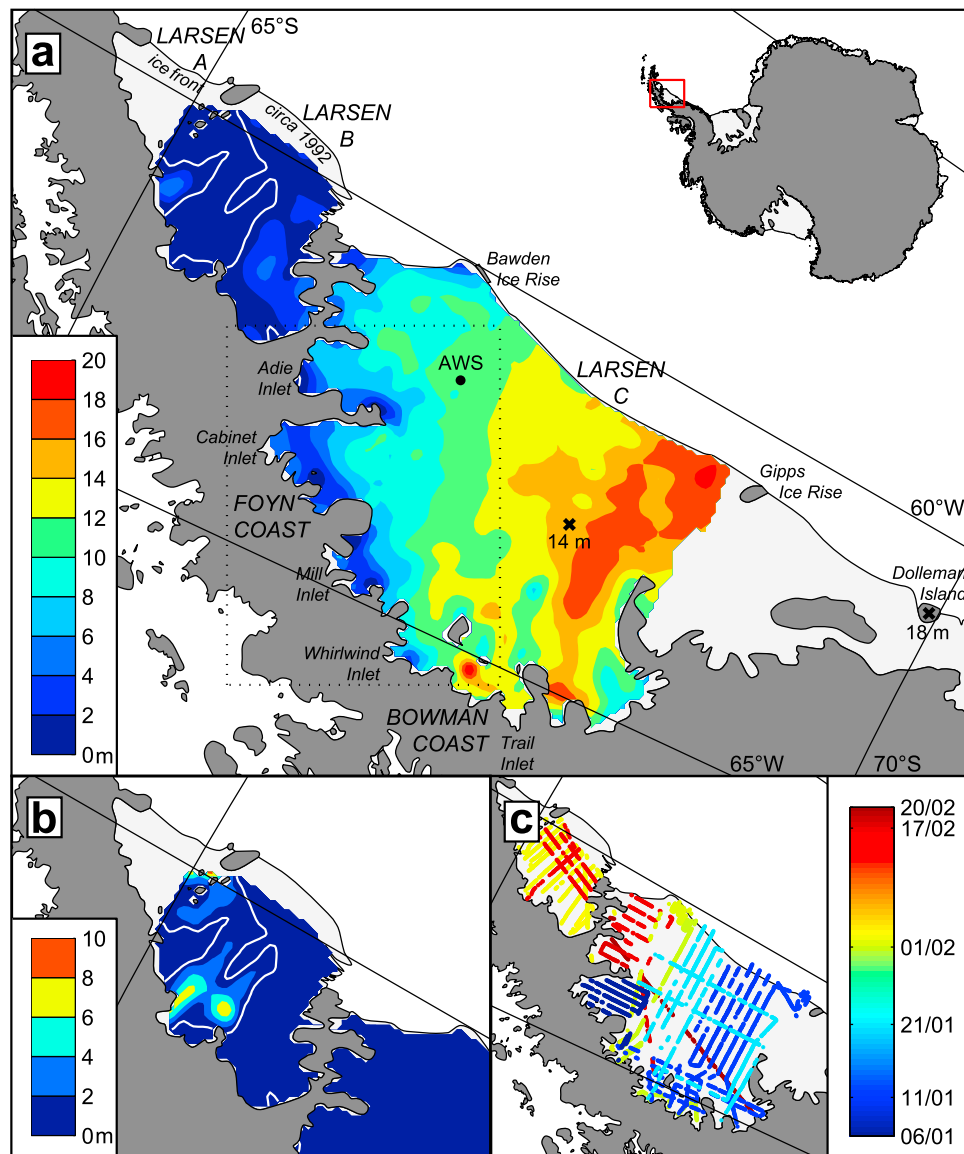


**Figure 1.** Results derived from 1997/98 survey data. (a) Air thickness derived by assuming dry firm (no water), (b) water thickness assuming saturated firm (no air), and (c) observation dates. In Figures 1a and 1b the white line marks the zero contour, beyond which negative values demonstrate that the assumption used must be incorrect. Figure 1a also shows in-situ air-thickness measurements and the Automatic Weather Station mentioned in the text. Figure 1b is cropped because negative water thicknesses are obtained throughout LCIS.

Measurements determine the left side of (3), but without additional information it is impossible to distinguish air from water. The square brackets show that the method is  $\sim 1.73$  times more sensitive to air (water's stronger influence on radar wave speed is overcome by its weaker effect on hydrostatic equilibrium), so any air thickness could be offset by a correspondingly larger water thickness. Here (3) is used to calculate air and ice thicknesses assuming  $W = 0$  and water and ice thicknesses assuming  $A = 0$ . These are limiting cases of cold dry firm and saturated temperate firm, and their accuracy in intermediate areas depends upon the location.

[6] The method is applied to British Antarctic Survey (BAS)–Instituto Antártico Argentino airborne data obtained from LIS in the 1997/98 austral summer [Holland *et al.*, 2009]. The survey used differential GPS and a radar

altimeter to obtain ice-shelf surface elevation and a radar transmitting a conventional  $0.25\text{-}\mu\text{s}$  pulse around 150 MHz to obtain through-ice travel-time. Surface elevations have the tidal signal removed (L. Padman, personal communication, 2010) and are adjusted to the EIGEN-GL04C geoid. No marine ice data contaminate the method because the RES failed to detect a base in marine bands [Holland *et al.*, 2009]. Hydrostatics is ensured by ignoring data within 2 km of land or marine ice and gridding the results at 2-km resolution, masked wherever further than 20 km from data and smoothed with 3 iterations of a 1-4-1 routine.

[7] Uncertainty in derived fields arises through error in instruments, processing datasets, assumptions, and parameters (Table 1). Raw surface elevations contain large absolute error (sea surface) and smaller random error (ice crossovers), which

**Table 1.** Error Associated With the Observations and Derived Quantities<sup>a</sup>

Quantity	RMS Error (m)
Ice-shelf travel-time crossovers (expressed as pure ice equivalent)	12.02
Raw ice surface elevation crossovers	1.82
Corrected ice surface elevation crossovers	1.24
Raw sea surface elevations	9.66
Corrected sea surface elevations	1.92
Dry firn air thickness crossovers	1.78
Dry firn ice thickness crossovers	13.29
Saturated firn water thickness crossovers	3.08
Saturated firn ice thickness crossovers	10.20

<sup>a</sup>Random error is quantified by crossovers (observations within 50 m of each other from different flights), while absolute surface error is quantified using observations of the sea surface (data with corrected elevations  $<5$  m). Tidal and geoid corrections significantly decrease random and absolute surface errors respectively.

are dramatically reduced by the geoid and tidal corrections respectively. Travel-time is picked manually and subject to instrument error. Fortunately, expressing travel-time as pure ice ( $T = 2In_i/c$ ), the left side of (3) shows that air thickness is  $\sim 9$  times more sensitive to elevation error than the larger travel-time error. Each density has uncertainty of  $\pm 2 \text{ kg m}^{-3}$ , combining to air thickness  $\pm 1$  m. Errors from (1) are limited as above, while (2) is compared with the widely used Looyenga formula [Endres *et al.*, 2009]; porosities differ by 10%, but the method mitigates this to air-thickness differences  $<0.1$  m.

### 3. Results

[8] Figure 1 shows LIS distributions of air (assuming dry firn) and water (saturated firn) calculated from (3). Negative values imply that the assumption used is incorrect; negative air (water) thickness implies the existence of some water (air). Figure 1a therefore reveals the presence of water in LBIS during the survey, whose derived thickness (Figure 1b) is a lower bound; if the firn were not saturated, water thickness would increase by  $\sim 1.73$  m for every 1 m of air remaining. Comparing Figures 1b and 1c shows that temporal variability in water content causes a lower value to be derived from later flights. Figure 1b confirms the existence of air in LCIS, rather than ruling out the presence of water; 1 m of water present during the survey would increase the air in Figure 1a by  $\sim 0.58$  m. Annual meltwater production at the LCIS Automatic Weather Station (Figure 1a) is  $\lesssim 0.4$  m [van den Broeke, 2005], so the error introduced by the presence of liquid water is  $\lesssim 0.2$  m if meltwater freezes every winter. Water content varies rapidly, so this error is included in the crossover analysis in Table 1. Figure 1a is therefore broadly correct for LCIS, though the high air content immediately north of Gippes Ice Rise is questionable because the ice is heavily rifted and not a floating continuum.

[9] The LCIS air map agrees with sparse available evidence. An ice core at Dolleman Island contained  $\sim 18$  m air (S. Cooper *et al.*, unpublished BAS field report R/1985–86/S4), and Jansen *et al.* [2010] derived a density profile containing  $\sim 14$  m air in southern LCIS (Figure 1a). Low

air thickness in northern LCIS and the presence of water in LBIS also agree with satellite observations. In LBIS, visible water ponding and low backscatter in synthetic aperture radar (SAR) imagery [Scambos *et al.*, 2003] suggest a wet-firn distribution that agrees with the extent of the derived water thicknesses. This area was lost in the 2002 LBIS collapse, suggesting that the method might help predict such events. Satellite images reveal melt ponds in the inlets along Foyen Coast that were present in 1997/98 (Figures 2a and 2b). Such meltwater will have densified firn in localized regions that clearly correspond to derived firn-air minima. Recent SAR images persistently show intense summer melting in these areas (Figure 2c) and low backscatter at the end of summer (Figure 2d) that probably reflects refrozen saturated firn (superimposed ice) [Scambos *et al.* 2003].

[10] These observations suggest that spatial variations in summer melting exert the greatest control on the distribution of firn air thickness. In warmer areas a larger proportion of the annual snow accumulation will melt and refreeze, changing from porous firn to solid ice. This imparts a spatial pattern to the air incorporated each year, so after several years the areas with persistently higher melting will have much less air in the ice column. Percolating meltwater causes additional densification by latent-heat release and the immersion of ice grains in water, so anomalous meltwater production could remove air accumulated over previous years. Spatial variations in precipitation could also affect air content, since a uniform melting would remove the air from a lower fraction of the yearly accumulation in high-precipitation areas, but there is no evidence for the increase in precipitation towards the southeast of LCIS that is required to explain the gradients in Figure 1a [van Lipzig *et al.*, 2004]. Surface temperature variations are much smaller than the  $\sim 20^\circ\text{C}$  required to cause a 10-m firn air change by dry compaction alone [Arthern *et al.*, 2010]. Therefore, we conclude that the derived air distribution reflects spatial variations in melting during the preceding years. This is supported by a reasonable anticorrelation ( $r = -0.65$ ) between the air data and gridded 1979/80–1997/98 mean number of melt days per year derived from passive microwave satellite measurements (Figure 3) [Tedesco, 2009].

[11] The firn air distribution and its apparent link to surface melting agree with our knowledge of LIS meteorology. Circumpolar westerly winds flow over the AP and descend its eastern side, causing increased melting in the lee (western LIS; Figures 1a and 3a) for several reasons [van Lipzig *et al.*, 2008]: rising air precipitates, so it is undersaturated and adiabatically warmed on its descent (the Föhn effect); dry descending air hosts fewer clouds, increasing shortwave radiation; and heat is advected eastwards across a climatological temperature gradient. Melting also increases to the north because the AP is lower, allowing a greater ‘flow-over’, and Coriolis force deflects Föhn winds northwards. The region is rapidly warming, which east of the AP is attributed to strengthening in the Southern Hemisphere Annual Mode (SAM) [Marshall *et al.*, 2006]. A higher SAM index is associated with stronger circumpolar westerlies causing more frequent flow-over, which increases both the surface sensible heat flux (Föhn effect) and incoming shortwave radiation (cloudiness) over the east and north of LCIS and all of LBIS [van Lipzig *et al.*, 2008]. 1979/80–2008/09 linear trends in melt days show a spatially-uniform increase

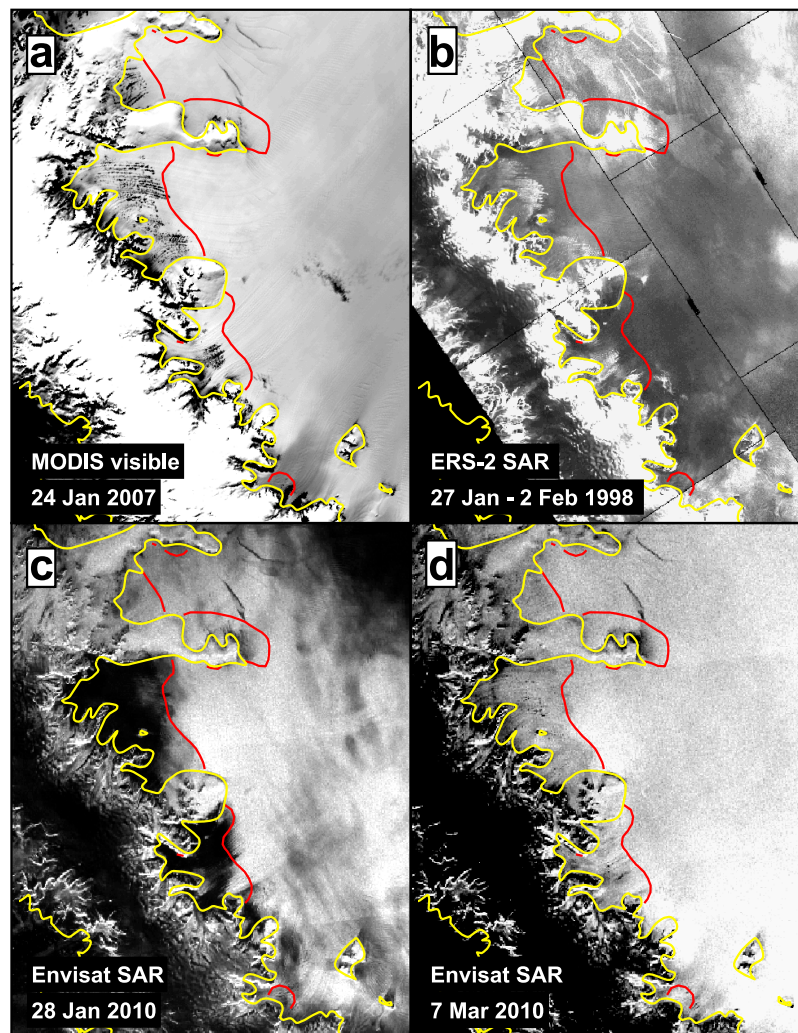


**Figure 2.** Satellite images of the Foyn Coast area of LCIS (dotted area in Figure 1a), with the grounding line shown in yellow and the 1997/98 6-m air contour in red. (a) Visible imagery clearly shows meltwater ponding in the inlets along Foyn Coast, suggesting intense meltwater-driven densification that accounts for the localized regions of low derived air thickness; (b) SAR imagery confirms that the melt ponds were present at the time of the 1997/98 survey (here refrozen and exhibiting high backscatter); (c) summer melting in the inlets persistently leads to a wet surface with low backscatter; (d) at the end of summer a superimposed ice region has low backscatter, providing a sharp contrast with the surrounding percolation zone [Scambos *et al.*, 2003].

of  $\sim 0.5$  melt days  $\text{a}^{-2}$ , or  $\sim 15$  extra melt days per year [Tedesco, 2009].

#### 4. Discussion

[12] Increased surface melting could control the lowering of LIS. The northern half of LCIS lowered by  $\sim 0.2 \text{ m a}^{-1}$  in 1992–2001 [Shepherd *et al.*, 2003] and 2003–2008 (P11); southern LCIS is broadly static. Figure 1a shows that in 1997/98 there was 8–12 m of air in the northern region, enough to support the lowering trend for decades. It is possible to use the spatial regression between firn air and melt days (Figure 3b) to suggest a temporal trend in firn air from the observed increase in melt days. This argument would only be correct if the firn instantly adjusted to changes in melting and the processes governing 1997/98 firn represented all those occurring over time. The spatial trend of  $0.4 \text{ m}$

(melt days  $\text{a}^{-1})^{-1}$  would explain a  $0.2 \text{ m a}^{-1}$  lowering by firn air loss arising from an increase of  $0.5$  melt days  $\text{a}^{-2}$ . This is similar to the trend reported by Tedesco [2009], though the uniform melting trend apparently does not match the pattern of surface lowering.

[13] The zero contour in Figures 1a and 1b is in reality the line at which the left side of (3) is zero because the increasingly positive effect of water on the right side exactly offsets the negative effect of the remaining air. Under the assumptions of dry and saturated firn this becomes the line of zero air and water. Scambos *et al.* [2003] suggest that meltwater ponding is necessary but not sufficient to drive collapse, which agrees with the observation that a section of LBIS was on the positive water/negative air side of the zero contour in 1997/98, long before it collapsed in 2002. If the LCIS lowering of  $0.2 \text{ m a}^{-1}$  were caused solely by air loss, and this trend were to continue, the area between Foyn Coast and



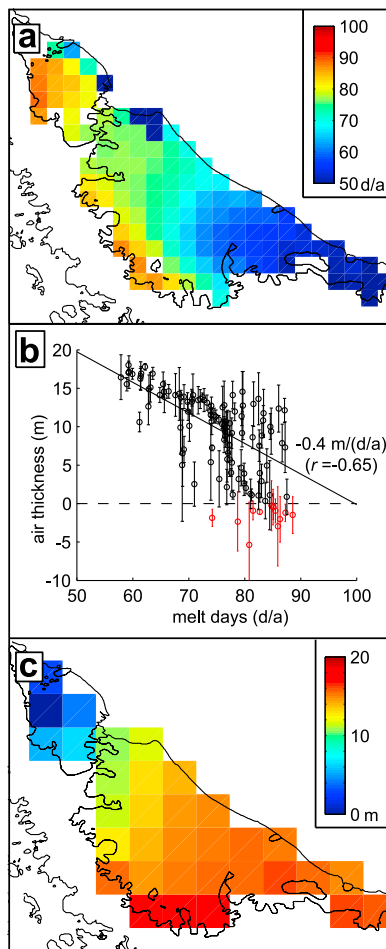


**Figure 3.** (a) 1979/80–1997/98 mean number of melt days per year [Tedesco, 2009], showing a strong inverse proportionality with the air thickness in Figure 1a everywhere except the Bowman Coast. (b) Spatial regression between air thickness and melt days per year (raw air-thickness data are binned at the resolution of the gridded melt days; bins that contain negative air thickness on average, red, are excluded from the regression). (c) Firm-air thickness predicted by a steady-state model that neglects melting [van den Broeke et al., 2008].

Bawden Ice Rise with 1997/98 air thickness <10 m would by 2050 be beyond the zero contour and in the same state of vulnerability to meltwater-driven collapse.

[14] These speculative conclusions do not by any means preclude a contribution to the lowering from oceanic basal melting, so the obvious next step is to repeat the measurements, determine changes in ice and air thicknesses, and distinguish the proportion of lowering caused by surface (air loss) and basal (ice loss) processes. However, change signals require time to exceed the combined uncertainties in the 1997/98 and repeat measurements. Given elevation error of ~1.25 m (Table 1) and a halved repeat error of 0.75 m, surface lowering of  $0.2 \text{ m a}^{-1}$  would be observable after 10 years (i.e., 2007/08). To ascribe this to surface melting requires  $0.2 \text{ m a}^{-1}$  air change, which with errors of ~1.75 m and 0.9 m emerges after ~13 years (2010/11). To ascribe it to basal melting, the hydrostatic ice-thickness change of  $1.8 \text{ m a}^{-1}$  emerges from errors of ~13 m and 7 m after ~11 years

(2008/09). An accurate repeat survey could already partition the lowering in areas of largest signal.

[15] The method presented here requires synoptic data, as shown by discrepancies within the LIS mission, and is sensitive to geoid error, which can be large in polar regions. It remains unable to discriminate air from water, though this might be resolved using additional properties of the RES return such as attenuation [Endres et al., 2009]. The method can use any RES data that are accompanied by accurate surface elevation measurements, and may also work using seismic sounding. It could create a climatology of firm air thickness, useful for calibrating firm models and deriving ice-shelf thickness from surface elevation data. Repeated measurements would allow air changes to be monitored, aiding the attribution of changes in surface elevation and allowing the conversion of changes in grounded ice discharge to mass and therefore sea-level [Rignot et al., 2008].

[16] Air thicknesses predicted by a coupled atmospheric and firm model [van den Broeke et al., 2008] agree rather well with our observations (Figures 3c and 1a), though as expected firm air is overpredicted in northern LCIS owing to the model's widely-acknowledged lack of melting. This explains a discrepancy between observed ice thicknesses and those derived from hydrostatic equilibrium using the model results [Griggs and Bamber, 2009]. It also has implications for studies that derive ice thickness change from surface elevation observations using firm models that neglect the potentially dominant melting change. Over a large LIS catchment, Helsen et al. [2008] showed a modeled firm thickness increase that exceeds the observed elevation increase for 1995–2003. The residual lowering implies either basal mass loss or a surface melting increase not captured in the firm correction. Using the same correction, Shepherd et al. [2010] found residual lowering for 1994–2008. Zwally et al. [2005] imply that their simpler firm model offsets all or half of the observed lowering for 1992–2001. The observational determination of firm air described here clearly holds great potential for such studies.

[17] **Acknowledgments.** The authors thank Daniel Grosvenor for correcting an error in the accepted manuscript.

[18] The Editor thanks two anonymous reviewers for their assistance in evaluating this paper.

## References

- Arcone, S. A. (2002), Airborne-radar stratigraphy and electrical structure of temperate firn: Bagley Ice Field, Alaska, U.S.A., *J. Glaciol.*, **48**, 317–334.
- Arthern, R. J., D. G. Vaughan, A. M. Rankin, R. Mulvaney, and E. R. Thomas (2010), In situ measurements of Antarctic snow compaction compared with predictions of models, *J. Geophys. Res.*, **115**, F03011, doi:10.1029/2009JF001306.
- Endres, A. L., T. Murray, A. D. Booth, and L. J. West (2009), A new framework for estimating englacial water content and pore geometry using combined radar and seismic wave velocities, *Geophys. Res. Lett.*, **36**, L04501, doi:10.1029/2008GL036876.
- Griggs, J. A., and J. L. Bamber (2009), Ice shelf thickness over Larsen C, Antarctica, derived from satellite altimetry, *Geophys. Res. Lett.*, **36**, L19501, doi:10.1029/2009GL039527.
- Helsen, M. M., et al. (2008), Elevation changes in Antarctica mainly determined by accumulation variability, *Science*, **320**, 1626–1629.
- Holland, P. R., H. F. J. Corr, D. G. Vaughan, A. Jenkins, and P. Skvarca (2009), Marine ice in Larsen Ice Shelf, *Geophys. Res. Lett.*, **36**, L11604, doi:10.1029/2009GL038162.
- Jansen, D., B. Kulessa, P. R. Sammonds, A. Luckman, E. C. King, and N. F. Glasser (2010), Present stability of the Larsen C Ice Shelf, Antarctic Peninsula, *J. Glaciol.*, **56**, 593–600.

- Marshall, G. J., A. Orr, N. P. M. van Lipzig, and J. C. King (2006), The impact of a changing Southern Hemisphere Annular Mode on Antarctic Peninsula summer temperatures, *J. Clim.*, *19*, 5388–5404.
- Rignot, E., et al. (2008), Recent Antarctic ice mass loss from radar interferometry and regional climate modelling, *Nat. Geosci.*, *1*, 106–110.
- Scambos, T., C. Hulbe, and M. Fahnestock (2003), Climate-induced ice shelf disintegration in the Antarctic Peninsula, in *Antarctic Peninsula Climate Variability: Historical and Paleoenvironmental Perspectives*, *Antarct. Res. Ser.*, vol. 79, edited by E. Domack et al., pp. 79–92, AGU, Washington, D. C.
- Shepherd, A. P., D. J. Wingham, A. J. Payne, and P. Skvarca (2003), Larsen Ice Shelf has progressively thinned, *Science*, *302*, 856–859.
- Shepherd, A., D. Wingham, D. Wallis, K. Giles, S. Laxon, and A. V. Sundal (2010), Recent loss of floating ice and the consequent sea level contribution, *Geophys. Res. Lett.*, *37*, L13503, doi:10.1029/2010GL042496.
- Tedesco, M. (2009), Assessment and development of snowmelt retrieval algorithms over Antarctica from K-band spaceborne brightness temperature (1979–2008), *Remote Sens. Environ.*, *113*, 979–997.
- van den Broeke, M. (2005), Strong surface melting preceded collapse of Antarctic Peninsula ice shelf, *Geophys. Res. Lett.*, *32*, L12815, doi:10.1029/2005GL023247.
- van den Broeke, M., W. J. van de Berg, and E. van Meijgaard (2008), Firn depth correction along the Antarctic grounding line, *Antarct. Sci.*, *20*, 513–517.
- van Lipzig, N. P. M., J. C. King, T. A. Lachlan-Cope, and M. R. van den Broeke (2004), Precipitation, sublimation, and snow drift in the Antarctic Peninsula region from a regional atmospheric model, *J. Geophys. Res.*, *109*, D24106, doi:10.1029/2004JD004701.
- van Lipzig, N. P. M., G. J. Marshall, A. Orr, and J. C. King (2008), The relationship between the Southern Hemisphere Annular Mode and Antarctic Peninsula summer temperatures, *J. Clim.*, *21*, 1649–1668.
- Zwally, H. J., et al. (2005), Mass changes of the Greenland and Antarctic ice sheets and shelves and contributions to sea level rise: 1992–2002, *J. Glaciol.*, *51*, 509–527.

---

R. J. Arthern, H. F. J. Corr, P. R. Holland, A. Jenkins, H. D. Pritchard, and D. G. Vaughan, British Antarctic Survey, High Cross, Madingley Road, Cambridge CB3 0ET, UK. (p.holland@bas.ac.uk)

M. Tedesco, Earth and Atmospheric Sciences, City College of New York, Marshak Science Building, New York, NY 10031, USA.